Supporting Information

Wrinkle facilitated hydrogen evolution reaction of vacancy-defected transition metal dichalcogenide monolayers

Mingjie Pu, Yufeng Guo* and Wanlin Guo#

State Key Laboratory of Mechanics and Control of Mechanical Structures and MOE Key Laboratory for Intelligent Nano Materials and Devices, College of Aerospace Engineering, Nanjing University of Aeronautics and Astronautics, Nanjing, 210016, China.

Corresponding Authors

*E-mail: yfguo@nuaa.edu.cn

E-mail: wlguo@nuaa.edu.cn

Table S1. The hydrogen adsorption Gibbs free energies ΔG_H of MoS_2 monolayers wrinkling along different directions, where a H atom adsorbs at the convex or concave part.

ΔG_H (eV)	Perfect-convex	Perfect-concave	V1-convex	V1-concave
Armchair	1.901	2.191	0.089	0.316
Zigzag	1.822	2.116	0.069	0.291

From Table S1, it is found that the hydrogen adsorption Gibbs free energy ΔG_H of wrinkling along zigzag direction is lower than that along armchair direction, hence only the wrinkles formed along the zigzag direction were considered in our work.

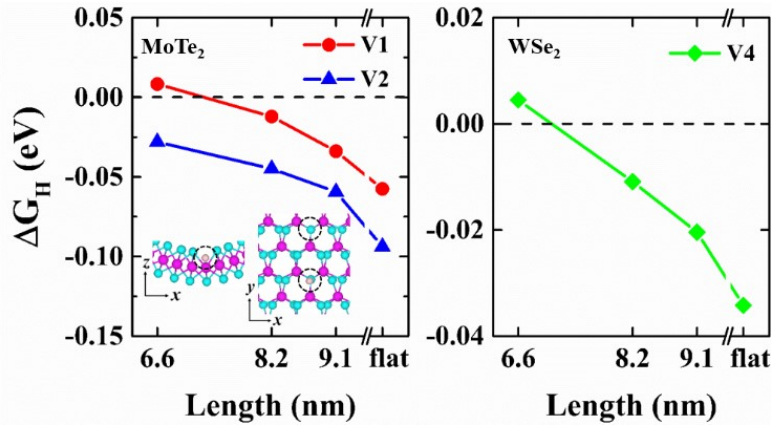

Figure S1. The hydrogen adsorption Gibbs free energies ΔG_H of wrinkled $MoTe_2$ and WSe_2 with vacancies formed at the concave parts under different wrinkle lengths. The inset shows the absorption site of a H atom at the concave part of $MoTe_2$.

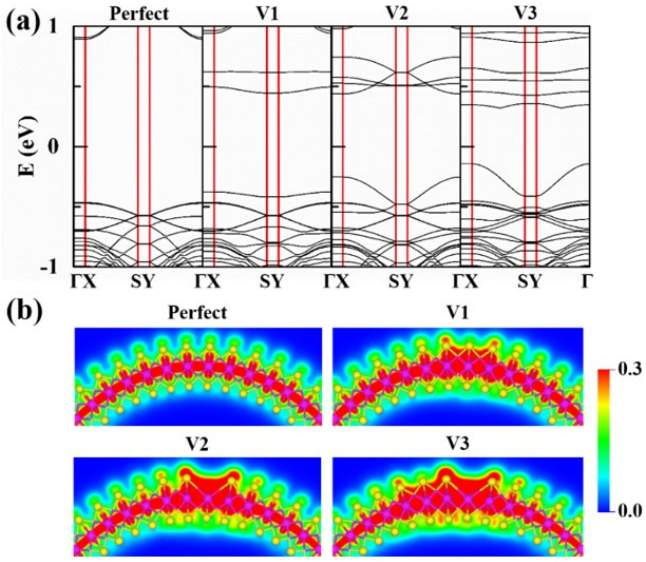

Figure S2. (a) Band structures of perfect and defected MoS_2 wrinkles with a length of 6.6 nm. (b) 2D projections of the partial charge densities (in units of $e \cdot Å^{-3}$) of the energy bands within the energy range from -1.0 eV to 1.0 eV for MoS_2 wrinkles. The Fermi level is set to be zero.

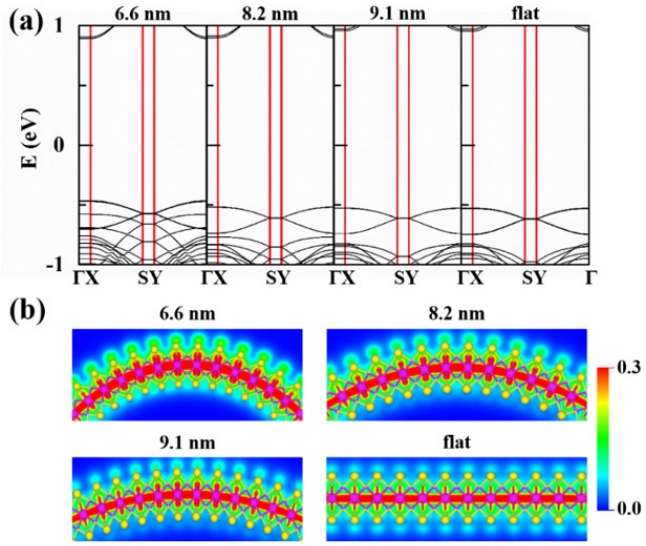

Figure S3. (a) Band structures of flat and wrinkled MoS_2 without defect. (b) 2D projections of the partial charge densities (in units of $e \cdot Å^{-3}$) of the energy bands within the energy range from -1.0 eV to 1.0 eV. The Fermi level is set to be zero.

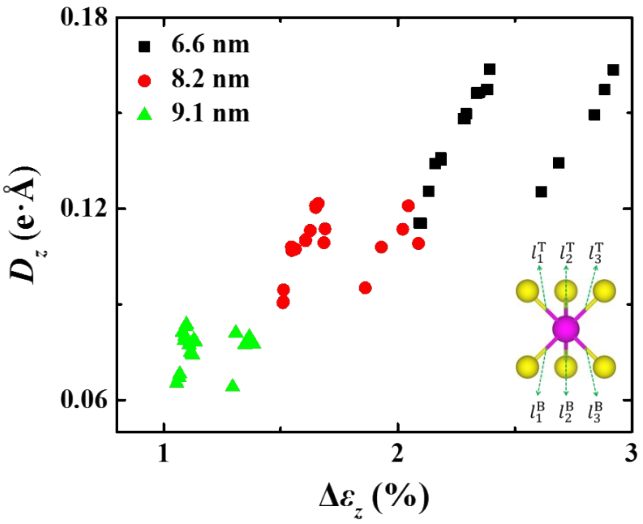

Figure S4. The *z*-direction dipole moments D_z of Mo atoms with strain gradient for perfect MoS_2 wrinkles with different wrinkle lengths. The inset shows the definition of Mo-S bonds on the top and bottom surfaces.

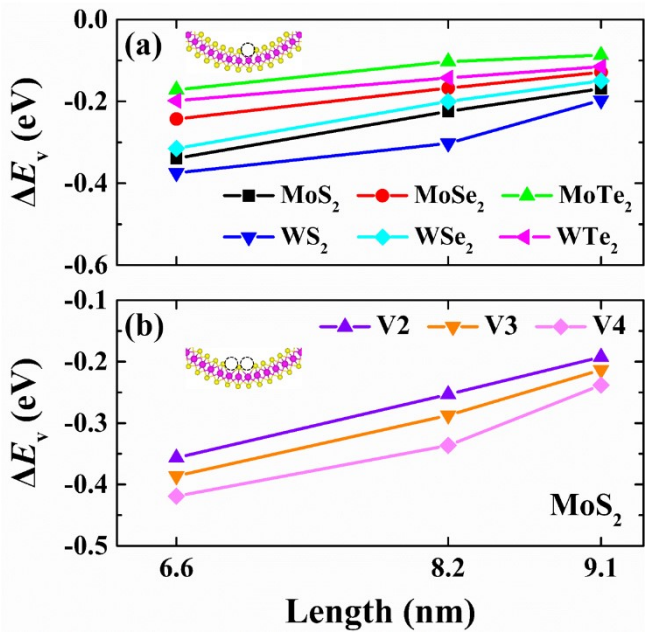

Figure S5. The vacancy formation energy differences ΔE_v of (a) wrinkled TMD MX_2 monolayers with one X-vacancy defect and (b) wrinkled MoS_2 monolayers with multiple vacancies formed at the concave parts under different wrinkle lengths. The insets shows the vacancy locations.

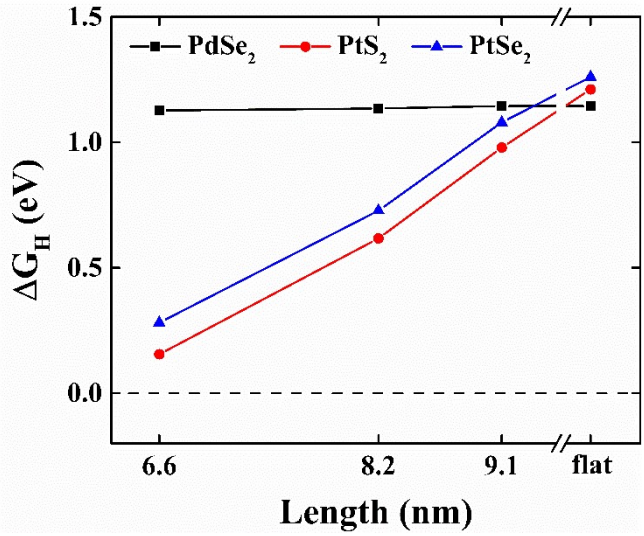

Figure S6. The hydrogen adsorption Gibbs free energies ΔG_H of monolayer $PdSe_2$, PtS_2 and $PtSe_2$ without defect under different wrinkle lengths.

The effect of wrinkling deformation on the hydrogen adsorption Gibbs free energies ΔG_H of monolayer $PdSe_2$, $PtSe_2$, PtS_2 without defect has been studied using the same method and procedure. As shown in Figure S6, the hydrogen adsorption Gibbs free energies of monolayer $PtSe_2$ and PtS_2 decrease with decreasing the wrinkle lengths, meaning that the HER of PtS_2 and $PtSe_2$ can be significantly improved by wrinkle engineering. However, ΔG_H of monolayer $PdSe_2$ is slightly affected by wrinkling deformation. When one vacancy defect is introduced in flat $PdSe_2$, ΔG_H decreases to 0.2657 eV. The combination of wrinkle engineering and defect engineering could be an effective way to improve the HER ability.